Tuning Subdivision Algorithms using Constrained Energy Optimization

I. Ginkel and G. Umlauf

Geometric Algorithms Group
Department of Computer Science
University of Kaiserslautern, Germany
ginkel|umlauf@informatik.uni-kl.de
http://www-umlauf.informatik.uni-kl.de

Abstract. In this paper a method is presented to fair the limit surface of a subdivision algorithm around an extraordinary point. The eigenvalues and eigenvectors of the subdivision matrix determine the continuity and shape of the limit surface. The dominant, sub-dominant and subsub-dominant eigenvalues should satisfy linear and quadratic equality- and inequality-constraints to guarantee continuous normal and bounded curvature globally. The remaining eigenvalues need only satisfy linear inequality-constraints. In general, except for the dominant eigenvalue, all eigenvalues can be used to optimize the shape of the limit surface with our method.

1 Introduction

Subdivision algorithms are a well established tool in computer graphics to model objects with free-form geometry. Nevertheless, the shape of the resulting subdivision surfaces have artifacts [24, 10]. This is one reason why subdivision surfaces are not widely used in CAD applications. Hence, there are various approaches to tune the subdivision algorithms to reduce these artifacts. Many approaches were taken that modify the differential geometric properties but not the fairness of the resulting subdivision surfaces [12, 3, 23, 8, 20, 21, 13, 6].

To further improve the fairness of the surfaces optimization techniques have been used to construct optimized stationary schemes. In [2] also the eigenvectors are modified by computing the stencils in an optimization process. The resulting subdivision algorithms approximate the desired eigenvector behavior. Based on the analysis in [10, 16] a different approach is presented in [1]. Here, the eigenvalues are determined such that the necessary conditions for bounded Gauss curvature are satisfied and the variation of curvature of the central surfaces in the shape chart is minimized. This is a non-linear optimization process which can only be approximated. It leads to subdivision algorithms with an eigenvalue distribution that approximately minimizes variation of Gauss curvature and the probability for a so-called hybrid shape. Nevertheless, in both approaches the immediate influence of the optimization on the fairness of the subdivision surface cannot be controlled directly.

The approaches taken in [7, 11] aim at fairing the limit surface. Instead to tune the respective subdivision algorithms they integrate optimization to the subdivision rules. The points of the fine control nets are computed such that a local or global energy functional is minimized. For both approaches this requires the solution of a global system of linear equations.

The principle of the tuning method presented here is based on a diagonalization of the subdivision matrix S. The eigenvalues of any stationary, linear and symmetric subdivision algorithm can be changed to satisfy the necessary conditions for bounded Gauss curvature using the technique described in [21]. This can be generalized to calculate the eigenvalue changes in an optimization process incorporating the necessary conditions as constraints imposing equality- and inequality-constraints on the dominant, sub-dominant and subsub-dominant eigenvalues of the subdivision matrix. The remaining eigenvalues must stay within certain intervals. Because the stencils depend linearly on the eigenvalues and a quadratic energy functional like the thin-plate energy depends quadratically on the control points, stencils can be computed that generate surfaces minimizing the respective functional. This means the scheme is no longer stationary, but it does not require the solution of a global system of equations.

The rest of the paper is structured into three sections. First the general concept of energy minimization for tuning subdivision surfaces is presented (Section 2). In Section 3 the constraints for the optimization process are derived from the Fourier analysis of subdivision schemes. These constraints include regularity, bounded curvature and changes that only affect the local neighborhood of the extraordinary point. The results of this method used to tune the algorithm of Catmull-Clark are shown in Section 4.

2 Energy minimization concept

A linear subdivision algorithm computes from a coarse initial net of control points $\mathcal{N}_0$ a refined net of control points $\mathcal{N}_1$ by taking finite affine combinations of control points of $\mathcal{N}_0$ to compute the control points of $\mathcal{N}_1$. This process is iterated to generate a sequence of control nets $(\mathcal{N}_r)_{r\geq 0}$ which converges to the subdivision surface.

For a primal subdivision algorithm the subdivision matrix S maps the k-ring neighborhood $\mathcal{C}_r, r \geq 0$, of an n-valent vertex $\mathbf{c}_r$ in $\mathcal{N}_r$ net to the k-ring neighborhood $\mathcal{C}_{r+1}$ of an n-valent vertex $\mathbf{c}_{r+1}$ in $\mathcal{N}_{r+1}$. Note that S is a square matrix and k depends on the size of the stencils. Each control net $\mathcal{C}_r$ defines a surface ring $\mathbf{x}_r$ which is represented as a linear combination of bi-variate, real valued, piecewise smooth functions $\mathbf{f} = [f_1, \ldots, f_l]$ forming a partition of unity corresponding to the column vector of control points C_r of $\mathcal{C}_r$

$$\mathbf{x}_r = \mathbf{f} \cdot C_r, \qquad r \geq 0.$$

Example surface rings are shown in Figure 1 for the algorithm of Catmull-Clark.

The goal of this paper is to construct a sequence of spline rings by a modified subdivision matrix $\widetilde{S}$, where each spline ring $\mathbf{x}_r$ has minimal energy $F(\mathbf{x}_r)$.

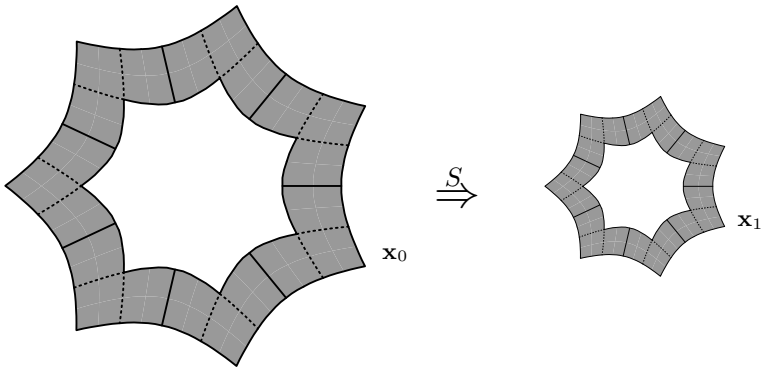

Fig. 1. Two consecutive surface rings $\mathbf{x}_0$ and $\mathbf{x}_1$ for the algorithm of Catmull-Clark at a 7-valent vertex.

If we take an energy functional like the thin-plate energy of a spline surface $\mathbf{x} : \mathbb{R}^2 \to \mathbb{R}^3$ with control points $\mathbf{p}_1, \ldots, \mathbf{p}_L \in \mathbb{R}^3$, it can be written as quadratic form, see e.g. [9]

$$F(\mathbf{x}) = \sum_{c=1}^{3} [\mathbf{p}_1^c, \ldots, \mathbf{p}_L^c] \cdot E \cdot [\mathbf{p}_1^c, \ldots, \mathbf{p}_L^c]^t,$$

where $\mathbf{p}_j^c$ denotes the c-th coordinate of control point $\mathbf{p}_j$. The matrix E contains the energies of the spline basis functions. If $\mathbf{f}$ consists of b-spline or box-spline functions, the surface rings $\mathbf{x}_r$ consist of s polynomial pieces as shown schematically in Figure 1 with $s = 3 \cdot 7$. The energy $F(\mathbf{x}_r)$ can then be computed as

$$F(\mathbf{x}_r) = \sum_{c=1}^{3} \sum_{j=1}^{s} (C_r^c)^t P_j^t E P_j C_r^c = \sum_{c=1}^{3} (C_r^c)^t \cdot \underbrace{\left(\sum_{j=1}^{s} P_j^t E P_j \right)}_{=: G} \cdot C_r^c,$$

where C_r^c denotes the column vector of c-th coordinates of the control points of C_r. The matrices P_j select those points from C_r that define the j-th patch of $\mathbf{x}_r$. Thus, the energy of $\mathbf{x}_{r+1}$ is given by

$$F(\mathbf{x}_{r+1}) = \sum_{c=1}^{3} (C_r^c)^t \widetilde{S}^t G \widetilde{S} C_r^c.$$

Since the optimization should be local, only a few stencils are modified, for example only the stencils for the extraordinary point and the control points in its one-ring neighborhood. If the control points are labeled circular around the extraordinary vertex as shown for the algorithm of Catmull-Clark in Figure 2(a),

the modified subdivision matrix $\widetilde{S}$ has the following structure

$$\widetilde{S} = \begin{bmatrix} \widetilde{S}_1 & 0 \\ S_2 & S_3 \end{bmatrix},$$

where $\widetilde{S}_1$ is the sub-matrix which contains the stencils that will be modified.

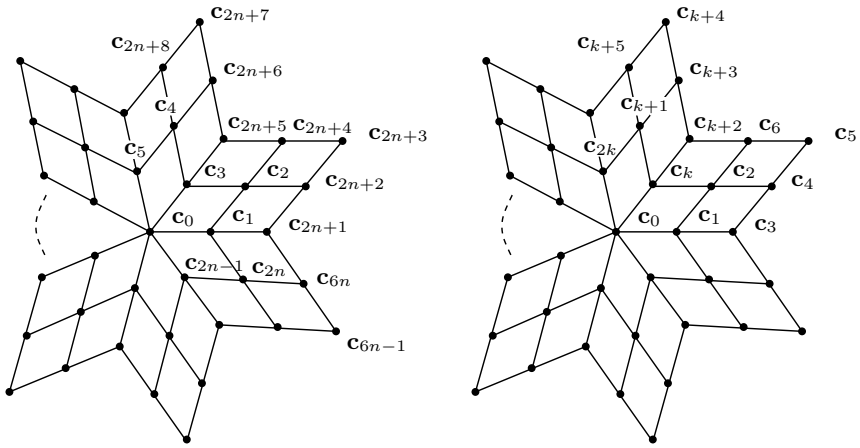

(a) *Circular labeling of the control points.*

(b) *Segmentwise labeling of the control points, where k is the number of points per segment.*

Fig. 2. Labeling of the control points around a vertex of valence n.

This structure is due to the fact that the stencils for the new positions of the extraordinary vertex and the one-ring are local. For the standard algorithms like the algorithms of Catmull-Clark or Loop S_1 is square. Thus, the energy $F(\mathbf{x}_r)$ can be written as

$$F(\mathbf{x}_{r+1}) = \sum_{c=1}^{3} (C_r^c)^t \left(\underbrace{\begin{bmatrix} \widetilde{S}_1 & 0 \\ 0 & 0 \end{bmatrix}}_{=:A} + \underbrace{\begin{bmatrix} 0 & 0 \\ S_2 & S_3 \end{bmatrix}}_{=:B} \right)^t G \left(\begin{bmatrix} \widetilde{S}_1 & 0 \\ 0 & 0 \end{bmatrix} + \begin{bmatrix} 0 & 0 \\ S_2 & S_3 \end{bmatrix} \right) C_r^c.$$

If $\widetilde{S}_1$ is diagonalizable, the eigenvalues of $\widetilde{S}_1$ can be used for optimization without affecting S_2 and S_3. To prepare the equations for the optimization we take a closer look at the matrix A, which contains the stencils that will be modified

$$AC_r^c = \begin{bmatrix} \widetilde{S}_1 & 0 \\ 0 & 0 \end{bmatrix} \begin{bmatrix} C_{1,r}^c \\ C_{2,r}^c \end{bmatrix} = \begin{bmatrix} \widetilde{S}_1 C_{1,r}^c \\ 0 \end{bmatrix}.$$

Denote by R the Matrix of eigenvectors of $\widetilde{S}_1$, by L its inverse with rows $\mathbf{w}_1, \ldots, \mathbf{w}_{l_1}$ and by D the diagonal matrix of the corresponding eigenvalues

$\lambda_1, \ldots, \lambda_{l_1}$ of $\widetilde{S}_1$. Then,

$$\begin{aligned}\widetilde{S}_1 C^c_{1,r} &= RDLC^c_{1,r} \\ &= R \begin{bmatrix} \lambda_1 & & \\ & \ddots & \\ & & \lambda_{l_1} \end{bmatrix} \begin{bmatrix} \mathbf{d}^c_1 \\ \vdots \\ \mathbf{d}^c_{l_1} \end{bmatrix} = R \begin{bmatrix} \mathbf{d}^c_1 & & \\ & \ddots & \\ & & \mathbf{d}^c_{l_1} \end{bmatrix} \begin{bmatrix} \lambda_1 \\ \vdots \\ \lambda_{l_1} \end{bmatrix} =: M^c_1 \boldsymbol{\lambda}_1,\end{aligned}$$

where $\mathbf{d}^c_i$ is the c-th coordinate of the so-called eigencoefficient $\mathbf{d}_i = \mathbf{w}_i C^c_{1,r}$, and

$$AC^c_r = \begin{bmatrix} M^c_1 & 0 \\ 0 & 0 \end{bmatrix} \begin{bmatrix} \boldsymbol{\lambda}_1 \\ 0 \end{bmatrix} =: M^c \boldsymbol{\lambda}.$$

Keeping R and L fixed, the energy $F(\mathbf{x}_{r+1})$ is quadratic in λ_i, since M^c and B do not depend on $\boldsymbol{\lambda}$, i.e.

$$\begin{aligned}F(\mathbf{x}_{r+1}) &= \sum_{c=1}^{3} (C^c_r)^t (A+B)^t G (A+B) C^c_r \\ &= \sum_{c=1}^{3} \left(\boldsymbol{\lambda}^t (M^c)^t G M^c \boldsymbol{\lambda} + 2 (C^c_r)^t B^t G M^c \boldsymbol{\lambda} + (C^c_r)^t B^t G B C^c_r \right). \quad (1)\end{aligned}$$

Using this representation of $F(\mathbf{x}_{r+1})$ the eigenvalues $\boldsymbol{\lambda}$ can be used for optimization with a prescribed number of stencils that will be modified.

3 Constrained energy minimization

To make the algorithm well-behaved we need certain constraints such as affine invariance or constraints that guarantee C^1 regularity of the limit surface. Many of these constraints become visible in the discrete Fourier analysis of the subdivision matrix.

Assume that the subdivision matrix S has only real eigenvalues $\lambda_1, \ldots, \lambda_l$ ordered by modulus

$$|\lambda_1| \geq \cdots \geq |\lambda_l| \geq 0$$

corresponding to the eigenvectors $\mathbf{v}_1, \ldots, \mathbf{v}_l$, i.e. $S\mathbf{v}_i = \lambda_i \mathbf{v}_i$ for $i = 1, \ldots, l$. If the subdivision algorithm uses only affine combinations, the dominant eigenvalue λ_1 is one and simple [19], i.e.

$$\lambda_1 = 1, \quad (2)$$

$$\lambda_1 > |\lambda_2|. \quad (3)$$

Then, the sequence of surface rings $(\mathbf{x}_r)_{r \geq 0}$ converges to the so-called extraordinary point $\mathbf{s}$ on the subdivision surface corresponding to $\mathbf{c}_0$.

If the subdivision algorithm is rotationally symmetric, the subdivision matrix S is block-circulant and similar to a block-diagonal matrix $\widehat{S}$ using the labeling of control points as in Figure 2(a)

$$S = \mathrm{circ}(S^0, \ldots, S^{n-1}) \sim \widehat{S} = \mathrm{diag}(\widehat{S}^0, \ldots, \widehat{S}^{n-1})$$

with the same eigenvalues, i.e. $\mathrm{spec}(S) = \bigcup_i \mathrm{spec}(\widehat{S}^i)$. Because $\widehat{S}$ is computed by a discrete Fourier transform as

$$\widehat{S}^i = \sum_{\ell=0}^{n-1} \omega_n^{-i\ell} S^\ell, \qquad \omega_n := \exp(2\pi\sqrt{-1}/n), i = 0, \ldots, n-1,$$

an eigenvalue ν of S is said to have Fourier index $\mathcal{F}(\nu)$ if $\nu \in \mathrm{spec}(\widehat{S}^{\mathcal{F}(\nu)})$. For subdivision surface to be regular and normal-continuous with bounded Gauss curvature of arbitrary sign at $\mathbf{s}$ the following conditions are sufficient ([22, 17]):

(i) The sub-dominant eigenvalue $\lambda_2 =: \lambda$ is a double, real eigenvalue and $\mathbf{v}_2, \mathbf{v}_3$ are linearly independent, i.e.

$$\begin{aligned} \lambda_2 &= \lambda_3, \\ |\lambda_2| &> |\lambda_4|, \ldots, |\lambda_l|. \end{aligned} \tag{4}$$

(ii) The so-called characteristic map $\mathbf{f} \cdot [\mathbf{v}_2 \mathbf{v}_3]$ is regular and injective.

(iii) The subsub-dominant eigenvalue $\lambda_4 =: \mu$ is real and satisfies

$$\mu = \lambda^2. \tag{5}$$

(iv) The subsub-dominant eigenvalue μ is a triple eigenvalue and $\mathbf{v}_4, \mathbf{v}_5, \mathbf{v}_6$ are linearly independent, i.e.

$$\lambda_4 = \lambda_5 = \lambda_6, \tag{6}$$

$$\lambda_4 > |\lambda_7|, \ldots, |\lambda_l|. \tag{7}$$

(v) The subsub-dominant eigenvalue μ has Fourier indices $0, 2$ and $n-2$.

The constraints (2)–(6) impose quadratic and linear equality- and inequality-constraints on the eigenvalues $\lambda_1, \ldots, \lambda_6$. The remaining eigenvalues $\lambda_i, i \geq 7$, can be chosen arbitrarily as long as (7) and Conditions (ii) and (v) are not violated. Combining the constraints with Equation (1) a quadratic equation with quadratic equality-constraints and linear inequality- and equality-constraints must be solved. Note that leaving the sub-dominant eigenvalues unchanged, the quadratic equality constraints disappear leading to a quadratic program.

4 Constrained energy minimization for the algorithm of Catmull-Clark

Using the labeling of control points as in Figure 2(b), the Fourier blocks $\widehat{S}^i, i = 0, \ldots, n-1$, of S of the algorithm of Catmull-Clark are given by

$$\widehat{S^i} = \left[\begin{array}{c|cc|ccc|ccccc}
\alpha\delta_{i,0} & \beta\delta_{i,0} & & \gamma\delta_{i,0} & & & & & & \\
\frac{3}{8}\delta_{i,0} & \frac{3}{8}+\frac{1}{8}c_i & & \frac{1}{16}+\frac{1}{16}\omega^{-i} & & & & & & \\
\frac{1}{4}\delta_{i,0} & \frac{1}{4}+\frac{1}{4}\omega^{i} & & \frac{1}{4} & & & & & & \\
\hline
\frac{3}{32}\delta_{i,0} & \frac{9}{16}+\frac{1}{32}c_i & \frac{3}{32}+\frac{3}{32}\omega^{-i} & \frac{3}{32} & \frac{1}{64} & 0 & \frac{1}{64}\omega^{-i} & & & \\
\frac{1}{16}\delta_{i,0} & \frac{3}{8}+\frac{1}{16}\omega^{i} & \frac{3}{8} & \frac{1}{16} & \frac{1}{16} & 0 & 0 & & & \\
\frac{1}{64}\delta_{i,0} & \frac{3}{32}+\frac{3}{32}\omega^{i} & \frac{9}{16} & \frac{1}{64}+\frac{1}{64}\omega^{i} & \frac{3}{32} & \frac{1}{64} & \frac{3}{32} & & & \\
\frac{1}{16}\delta_{i,0} & \frac{1}{16}+\frac{3}{8}\omega^{i} & \frac{3}{8} & \frac{1}{16}\omega^{i} & 0 & 0 & \frac{1}{16} & & & \\
\hline
0 & \frac{3}{8} & \frac{1}{16}+\frac{1}{16}\omega^{-i} & \frac{3}{8} & \frac{1}{16} & 0 & \frac{1}{16}\omega^{-i} & 0 & 0 & 0 & 0 & 0 & 0 \\
0 & \frac{1}{4} & \frac{1}{4} & \frac{1}{4} & \frac{1}{4} & 0 & 0 & 0 & 0 & 0 & 0 & 0 & 0 \\
0 & \frac{1}{16} & \frac{3}{8} & \frac{1}{16} & \frac{3}{8} & \frac{1}{16} & \frac{1}{16} & 0 & 0 & 0 & 0 & 0 & 0 \\
0 & 0 & \frac{1}{4} & 0 & \frac{1}{4} & \frac{1}{4} & \frac{1}{4} & 0 & 0 & 0 & 0 & 0 & 0 \\
0 & \frac{1}{16}\omega^{i} & \frac{3}{8} & \frac{1}{16}\omega^{i} & \frac{1}{16} & \frac{1}{16} & \frac{3}{8} & 0 & 0 & 0 & 0 & 0 & 0 \\
0 & \frac{1}{4}\omega^{i} & \frac{1}{4} & \frac{1}{4}\omega^{i} & 0 & 0 & \frac{1}{4} & 0 & 0 & 0 & 0 & 0 & 0
\end{array}\right],$$

where $\omega := \exp(2\pi\sqrt{-1}/n)$, $c_i := \cos(2\pi i/n)$ and the Kronecker symbol $\delta_{i,0}$. From $\widehat{S}^i$ the eigenvalues of S can be computed as:

- the eigenvalue $\lambda_0 = 1$ from $\widehat{S}_0$,
- the eigenvalues $\mu_\alpha^\pm := (4\alpha - 1 \pm \sqrt{(4\alpha-1)^2 + 8\beta - 4})/8$ from $\widehat{S}_0$,
- the eigenvalues $\mu_i^\pm := (5 + c_i \pm \sqrt{(c_i+9)(c_i+1)})/16$ from $\widehat{S}_i, i = 1, \ldots, n-1$,
- the n-fold eigenvalues $\frac{1}{8}, \frac{1}{16}, \frac{1}{32}, \frac{1}{64}$ from $\widehat{S}_i, i = 0, \ldots, n-1$,
- the $(7n-1)$-fold eigenvalue 0 from $\widehat{S}_i, i = 0, \ldots, n-1$.

The upper left 3×3 block of $\widehat{S}_i$ corresponds to the extraordinary vertex and its one-ring neighborhood. Diagonalizing this block, its eigenvalues can be used for optimization subject to the following constraints:

$$\lambda_0 = 1, \tag{8}$$

$$1/\sqrt{8} < \mu_1^+ < 1, \tag{9}$$

$$\mu_\alpha^+ = \mu_2^+ = (\mu_1^+)^2, \tag{10}$$

$$\mu_i^+ = \mu_{n-i}^+ \text{ and } \mu_i^- = \mu_{n-i}^- \text{ for } i = 1, \ldots, \lfloor n/2 \rfloor, \tag{11}$$

$$|\mu_\alpha^-|, |\mu_i^\pm|, |\mu_1^-|, |\mu_2^-| < \mu_2^+ \text{ for } i = 3, \ldots, \lfloor n/2 \rfloor. \tag{12}$$

The results of an optimization with these contraints using the libraray [14] are shown in Figures 5 . The control nets shown in Figure 3 contain irregular vertices of valence 7 and 11. It does not seem necessary to hold up the triple subsubdominant eigenvalue, since hybrid shapes can still occur (see Figure 5 bottom left). Instead we replace the constraints $\mu_2^+ = (\mu_1^+)^2$ by $|\mu_2^+| < (\mu_1^+)^2$ for elliptic and $\mu_\alpha^+ = (\mu_1^+)^2$ by $|\mu_\alpha^+| < (\mu_1^+)^2$ for hyperbolic shapes. We leave the decision whether the shape is going to be elliptic or hyperbolic to the optimization by calculating both variants and taking the one that produces lower energy for the spline rings, see Figure 4 and Figure 5 bottom right.

The functional that has been used for the optimization is

$$F(\mathbf{x}) = \int_{[0,1]^2} \left(\mathbf{x}_{uuu}^2 + 3\mathbf{x}_{uuv}^2 + 3\mathbf{x}_{uvv}^2 + \mathbf{x}_{vvv}^2\right) du\, dv, \tag{13}$$

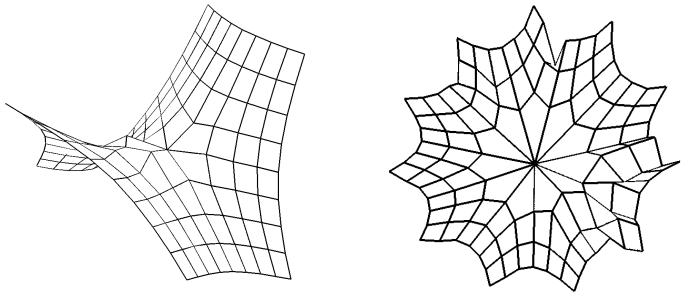

(a) *Control net with an irregular vertex of valence* 7.

(b) *Control net with an irregular vertex of valence* 11.

Fig. 3. Two different control nets for the algorithm of Catmull-Clark.

where $\mathbf{x}_u$ and $\mathbf{x}_v$ denote the partial derivatives of $\mathbf{x}$ with respect to u and v. We chose a parameterization dependent third order measure as a reasonable approximation to the variation of curvature. Since second order measures may lead to flat surfaces, minimizing the variation of curvature rather than its magnitude leads to fairer and more pleasing surfaces [15].

The influence of the optimization is visible in the visualization of the Gauss curvature. For the surface in Figure 4, we additionally document the tendency towards a hyperbolic configuration in Table 1. It shows the optimized values for μ_α^+, μ_2^+ and μ_{n-2}^+ for the first 8 subdivision steps and compares the energies of the innermost two spline rings at the corresponding subdivision level with and without optimization.

r	μ_α^+	μ_2^+, μ_{n-2}^+	$F(\mathbf{x})$ without optimization	$F(\mathbf{x})$ with optimization
1	0.365611	0.365768	28.08448	25.96919
2	0.354541	0.355186	7.112990	6.828013
3	0.347269	0.350177	2.246211	2.192127
4	0.345149	0.348187	0.751045	0.736397
5	0.341162	0.347430	0.256974	0.252283
6	0.337389	0.347161	0.088712	0.087122
7	0.324970	0.347065	0.030727	0.030179
8	0.203355	0.347033	0.010656	0.010466

Table 1. Optimized values for μ_α^+,μ_2^+, μ_{n-2}^+ and comparision of the energies of the innermost two spline rings at the corresponding subdivision level r with and without optimization for the algorithm of Catmull-Clark for the surfaces in Figure 4.

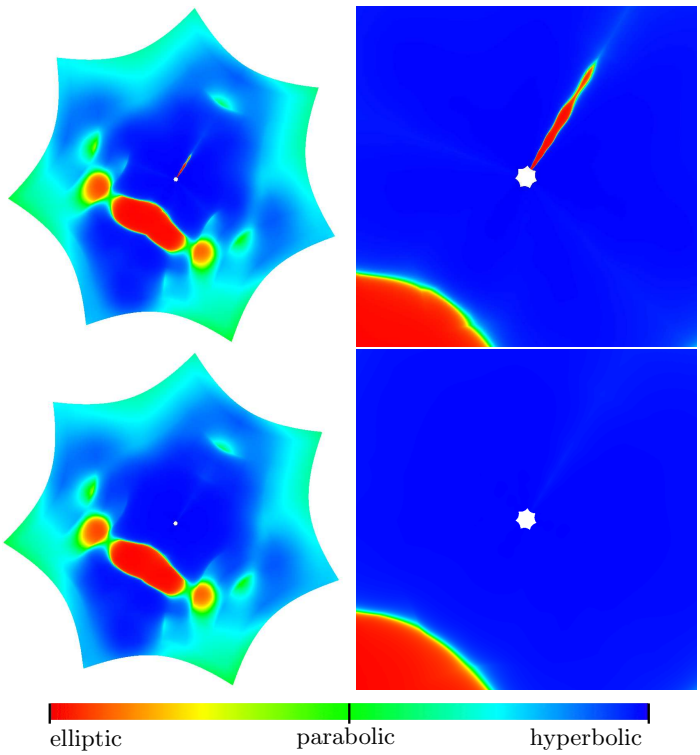

Fig. 4. Comparison of two different subdivision surfaces corresponding to the control net in Figure 3(a) after 8 subdivision steps. *Top*: Modified Catmull-Clark algorithm ([20]) with bounded curvature of arbitrary sign. *Bottom*: Optimized Catmull-Clark algorithm with double subsub-dominant eigenvalue for hyperbolic shape. The right column shows the corresponding zoom at the extraordinary point. For color images please refer to our website.

Remark 1. Changes in the stencils for the one-ring around the extraordinary vertex by the optimization influence the spline rings $\mathbf{x}_{r+1}$ and $\mathbf{x}_r$. Therefore, the optimization has to take both rings into account by choosing the size of C_r, S and G such that four rings of control points are used in the optimization.

Remark 2. Since the optimization changes μ_1^+, the proof for regularity and injectivity of the characteristic map is no longer valid. It needs to be re-done using the technique in [25] for the new choice of μ_1^+.

5 Conclusion

We have presented a technique to tune subdivision algorithms using constrained energy optimization. This allows to obtain bounded curvature for the limit behavior in combination with a fair shape around the extraordinary point.

As future work we will determine an interval of valid values for μ_1^+, for which the characteristic map is regular and injective. This interval would be included into the optimization as further constraint.

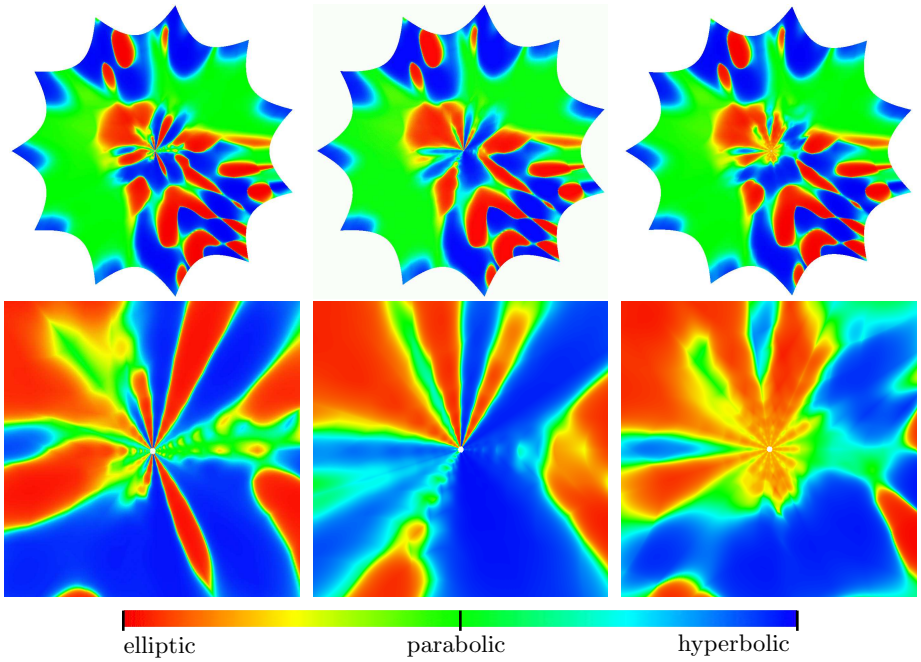

Fig. 5. Comparison of three different subdivision surfaces corresponding to the control net in Figure 3(b) after 12 subdivision steps. *Left*: Modified Catmull-Clark algorithm ([20]) with bounded curvature of arbitrary sign. *Middle*: Optimized Catmull-Clark algorithm with triple subsub-dominant eigenvalue. *Right*: Optimized Catmull-Clark algorithm with single subsub-dominant eigenvalue for elliptic shape. The top row shows the surface and the bottom row shows the corresponding zoom at the extraordinary point. For color images please refer to our website.

References

1. U. Augsdörfer, N.A. Dodgson and M.A. Sabin, A new way to tune subdivision, in *Eurographics Symposium on Geometry Processing*, M. Desbrun and H. Pottmann eds. (2005).
2. L. Barthe and L. Kobbelt, Subdivision scheme tuning around extraordinary vertices, *Comput. Aided Geom. Design* **21** (2004) 561–583.
3. E. Catmull and J. Clark, Recursive generated B-spline surfaces on arbitrary topological meshes, *Comput.-Aided Des.* **10** (1978) 350–355.

4. D.W.H. Doo and M. Sabin, Behaviour of recursive division surfaces near extraordinary points, *Comput.-Aided Des.* **10** (1978) 356–360.
5. I. Ginkel and G. Umlauf, Analyzing a generalized Loop subdivision scheme, to appear: Computing, 2006.
6. I. Ginkel and G. Umlauf, Loop subdivision with curvature control. *Eurographics Symposium on Geometry Processing*, K. Polthier and A. Sheffer eds. (2006) 163-171.
7. M.A. Halstead, M. Kass, and T.D. DeRose, Efficient, fair interpolation using Catmull-Clark surfaces, *SIGGRAPH '93* pp. 35–44 (1993).
8. F. Holt, Towards a curvature-continuous stationary subdivision algorithm, *Z. Angew. Math. Mech.* **76** (1996) 423–424.
9. M. Kallay, Constrained optimization in surface design, in *Modeling in Computer Graphics*, B. Falcidieno and T. L. Kunii eds. (Springer, 1993), 85–93.
10. K. Karciauskas, J. Peters and U. Reif, Shape characterization of subdivision surfaces – case studies, *Comput. Aided Geom. Design* **21** (2004) 601–614.
11. L. Kobbelt, A variational approach to subdivision, *Comput. Aided Geom. Design* **13** (1996) 743–761.
12. C. Loop, Smooth subdivision surfaces based on triangles, Master Thesis, University of Utah (1987).
13. C. Loop, Bounded curvature triangle mesh subdivision with the convex hull property, *Visual Comput.* **18** (2002) 316–325.
14. J. C. Meza, R. A. Oliva, P. D. Hough, and P. J. Williams, OPT++: An Object-Oriented Class Library for Nonlinear Optimization.
15. H. Moreton and C. Séquin, Minimum Variation Curves and Surfaces for Computer-Aided Geometric Design, in *Designing fair Curves and Surfaces*, N.S. Sapidis ed. SIAM, Philadelphia (1994), 123–159.
16. J. Peters and U. Reif, Shape characterization of subdivision surfaces – basic principles, *Comput. Aided Geom. Design* **21** (2004) 585–599.
17. J. Peters and G. Umlauf, Gaussian and mean curvature of subdivision surfaces, in *The Mathematics of Surfaces IX*, R. Cipolla and R. Martin eds. (Springer, 2000) pp. 59–69.
18. H. Prautzsch, Smoothness of subdivision surfaces at extraordinary points, *Adv. Comput. Math.* **9** (1998) 377–389.
19. H. Prautzsch, W. Boehm and M. Paluszny, *Bézier and B-Spline Techniques*, Springer (2002).
20. H. Prautzsch and G. Umlauf, A G^2-subdivision algorithm, *Computing* **13** (1998) 217–224.
21. H. Prautzsch and G. Umlauf, A G^1 and G^2 subdivision scheme for triangular nets, *Int. J. Shape Model.* **6** (2000) 21–35.
22. U. Reif, A unified approach to subdivision algorithms near extraordinary vertices, *Comput. Aided Geom. Design* **12** (1995) 153–174.
23. M.A. Sabin, Cubic recursive division with bounded curvature, in P.J. Laurent, A. Le Méhauté and L.L. Schumaker eds., *Curves and Surfaces* (Academic Press, 1991) pp. 411–414.
24. M.A. Sabin and L. Barthe, Artifacts in recursive subdivision surfaces, in *Curve and Surface Fitting – Saint-Malo 2002*, A. Cohen, J.-L. Merrien, and L.L. Schumaker eds. (Nashboro Press, 2003) pp. 353–362.
25. G. Umlauf, A technique for verifying the smoothness of subdivision schemes, in *Geometric Modeling and Computing*, M.L. Lucian and M. Neamtu eds. (Nashboro Press, 2004), 513–521.